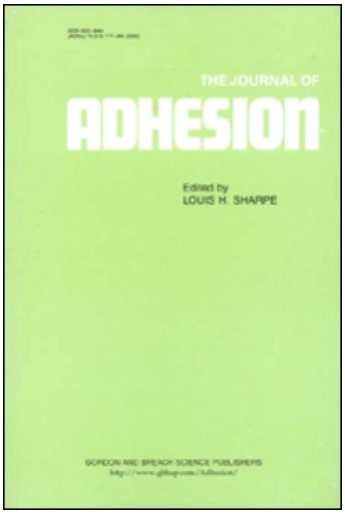

The Journal of Adhesion

Publication details, including instructions for authors and subscription information:
http://www.informaworld.com/smpp/title~content=t713453635

Time-Dependence of Epoxy Debonding

Douglas B. Adolf[a]; Mark E. Stavig[a]; Stacie Kawaguchi[a]; Robert S. Chambers[b]
[a] Materials and Process Sciences Center, Sandia National Laboratories, Albuquerque, New Mexico, USA [b] Engineering Sciences Center, Sandia National Laboratories, Albuquerque, New Mexico, USA

To cite this Article Adolf, Douglas B. , Stavig, Mark E. , Kawaguchi, Stacie and Chambers, Robert S.(2007) 'Time-Dependence of Epoxy Debonding', The Journal of Adhesion, 83: 1, 85 — 104
To link to this Article: DOI: 10.1080/00218460601102886
URL: http://dx.doi.org/10.1080/00218460601102886

The Journal of Adhesion, 83:85–104, 2007

ISSN: 0021-8464 print/1545-5823 online
DOI: 10.1080/00218460601102886

Taylor & Francis
Taylor & Francis Group

Time-Dependence of Epoxy Debonding

Douglas B. Adolf
Mark E. Stavig
Stacie Kawaguchi
Materials and Process Sciences Center, Sandia National Laboratories, Albuquerque, New Mexico, USA

Robert S. Chambers
Engineering Sciences Center, Sandia National Laboratories, Albuquerque, New Mexico, USA

Test geometries with well-defined stresses at the initiation of adhesive failure (failure in adhesion) were used to examine debonding of epoxies in controlled ramp and creep tests. Little effect of substrate, curative, or filler content was seen in failure initiation for the variations studied. The time-to-fail in creep tests depended sensitively on the applied load. Sinusoidal shear loads were also applied in both single (zero to max) and double-sided (−max to + max) mode. Whereas the single-sided, oscillatory loaded samples failed much later than samples loaded in creep to the same maximum stress, double-sided times-to-fail were similar to those in creep.

Keywords: Adhesion; Creep; Debonding; Epoxy; Oscillatory; Time-dependence

1. INTRODUCTION

Butt tensile and lap shear tests are typically used to compare the strength of different adhesive bonds. Although the stresses in these geometries are often erroneously assumed to be homogeneous, the true stress fields are so concentrated at corners that failure can be

Received 8 September 2006; in final form 31 October 2006.

Sandia is a multiprogram laboratory operated by Sandia Corporation, a Lockheed Martin Company, for the U.S. Department of Energy's National Nuclear Security Administration under Contract DE-AC04-94AL85000.

Address correspondence to Douglas B. Adolf, Materials and Process Sciences Center, Sandia National Laboratories, Albuquerque, NM 87185-0888, USA. E-mail: dbadolf@sandia.gov

analyzed *via* fracture mechanics approaches [1]. In electronic components encapsulated with polymer, however, interfacial debonding may not be associated with such intense stress risers. Initial debonding may, in fact, occur at as-designed adhered surfaces embedded within the component where there are relatively benign radii of curvatures and no apparent surface cracks. Although fracture mechanics approaches are inapplicable in such situations, stresses and strains may be calculated fairly accurately, and the initiation of debonding might be predicted by a critical magnitude of the surface traction.

A laboratory test is required in which stresses and strains are relatively smoothly varying at the initiation site (unlike butt tensile and lap shear) such that the critical surface tractions can be extracted. Examples of such lab tests are the napkin-ring [2] and the cruciform [3] geometries, which enable measurement of the critical shear and tensile surface tractions, respectively. In a previous paper [4], we presented a saucer test geometry that also avoided stress risers and enabled determination of critical surface tractions in shear, tension, and mixed modes of deformation. This sample was used to determine the critical tractions for initiating adhesive failure (failure in adhesion) at interfaces in ramped strain tests as a function of test temperature.

In the current article, test procedures and results from this previous study are reviewed briefly, and new results from ramped strain tests on epoxies are presented that examine the dependence of the critical tractions on the type of polymer, substrate, and filler additive. More interestingly, results are presented from creep tests that ramp to a load less than critical (defined as the load-to-fail in a ramp test) and maintain that load. The samples fail in time, taking longer to debond as the applied load strays farther from the critical load. Finally, the time dependence for debonding is examined for sinusoidally varying loads.

2. CRITICAL TRACTIONS FROM STRAIN RAMP TESTS

The new saucer geometry is pictured in Figures 1 and 2. The dimensions and radii of curvature were designed using finite element analysis [4] to ensure that (1) adhesive failure initiates away from an air interface, (2) the stress distribution near the initiation site is slowly varying, (3) the thermal residual stresses are not dominant, and (4) mixed-mode testing is enabled. Stresses in the strain-controlled, monotonically ramped tests were calculated using an accurate, nonlinear, viscoelastic, constitutive equation developed and validated in previous publications [5,6]. The epoxy adhesive consisted of 100 parts by weight of the digylcidyl ether of bisphenol A (DGEBA, Resolution

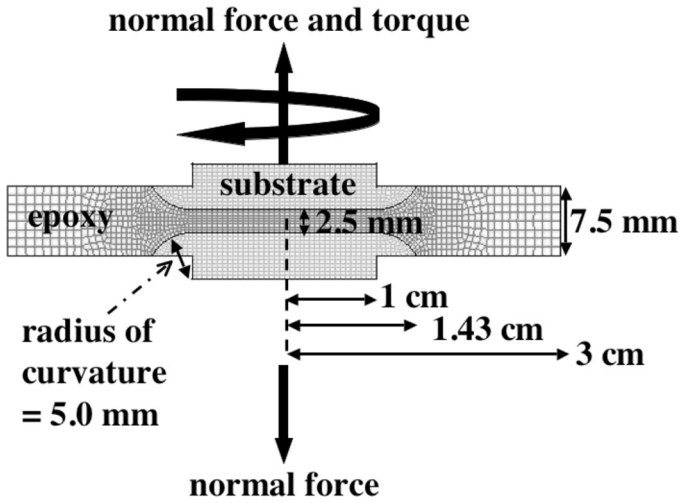

FIGURE 1 Schematic of the new saucer geometry for adhesion tests.

Epon 828, Houston, TX, USA) cured with 12 parts by weight diethanolamine (DEA, Fisher Scientific, Hampton, NH, USA) at 90°C for 48 h. All substrate surfaces examined after testing appeared consistent with adhesive failure. Monotonically ramped tensile tests were conducted

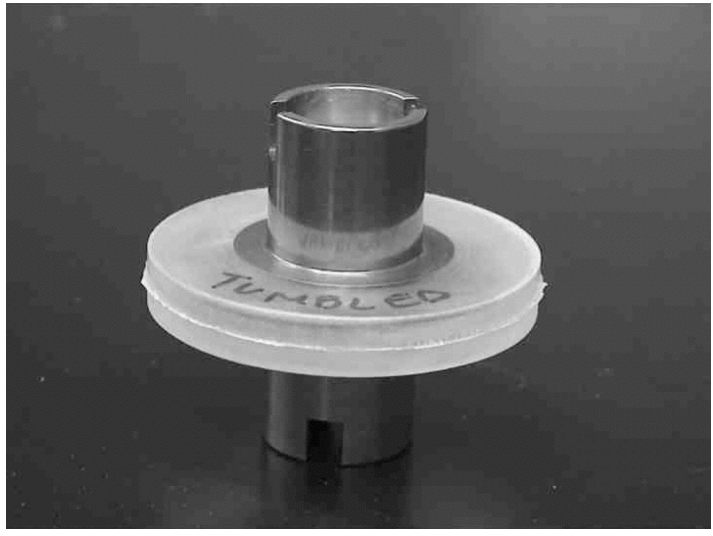

FIGURE 2 Photograph of the new saucer geometry for adhesion tests.

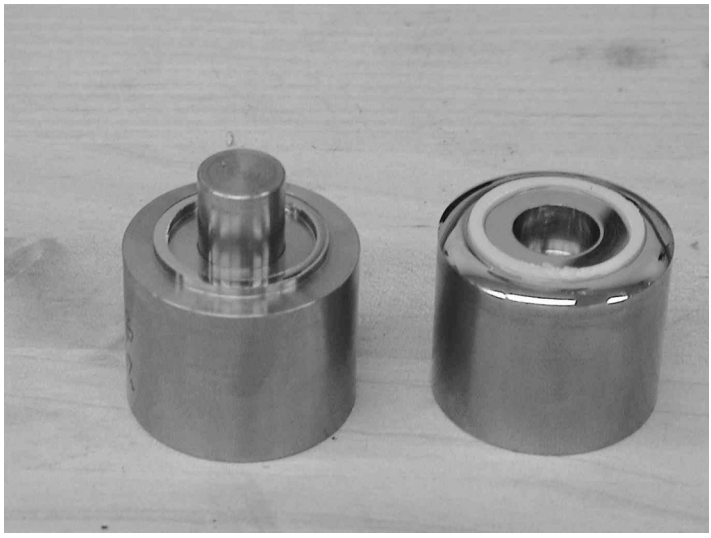

FIGURE 3 Photograph of the napkin-ring geometry for adhesion tests.

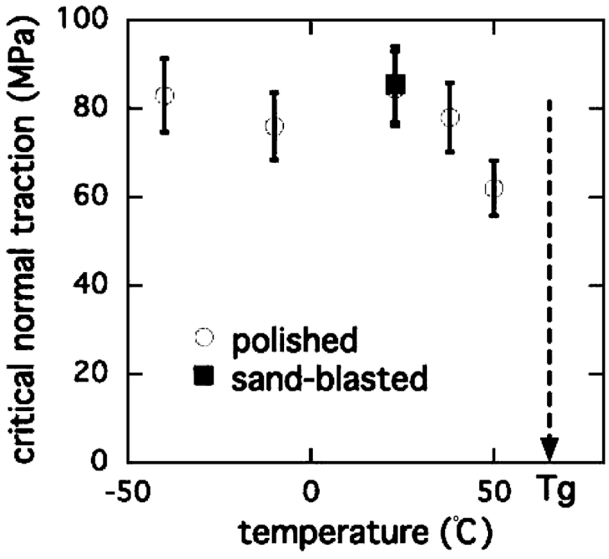

FIGURE 4 Temperature dependence of the critical normal traction for debonding using the saucer geometry with either polished or sand-blasted surface finishes.

on an Instron (Norwood, MA, USA) 1125 axial load frame at a rate of 1.27 mm/min. Monotonically ramped torsional tests were conducted on an axial/rotational Instron load frame at a rate of 5 degrees/min. More details are presented in Ref. 4.

Several tests in shear were reproduced using the napkin-ring geometry pictured in Figure 3. The lower face (on the right in Figure 3) was simply a flat, stainless steel (type 304) plug 25.4 mm in diameter. The upper face (upside down on the left in Figure 3) had a 16.5-mm I.D./19-mm O.D. ring machined onto the flat, stainless steel plug. A nominal 0.5-mm adhesive gap was held constant during cure by a spacer (the cylinder in the middle of the upper plug in Figure 3) that could be adjusted with a screw through the lower plug. This screw was backed off after cure so the spacer added no frictional force during the test. Monotonically ramped torsional tests were run on an Instron axial/torsional load frame at a rate of 5 degrees/min. Adhesive failures always initiated on the top surface. The white, filled epoxy in Figure 3 is almost intact on the lower plug after testing.

Previous results [4] investigated the temperature dependence of the critical tensile and shear tractions (Figures 4 and 5) at the initiation of adhesive failure. Although the critical tensile tractions appear

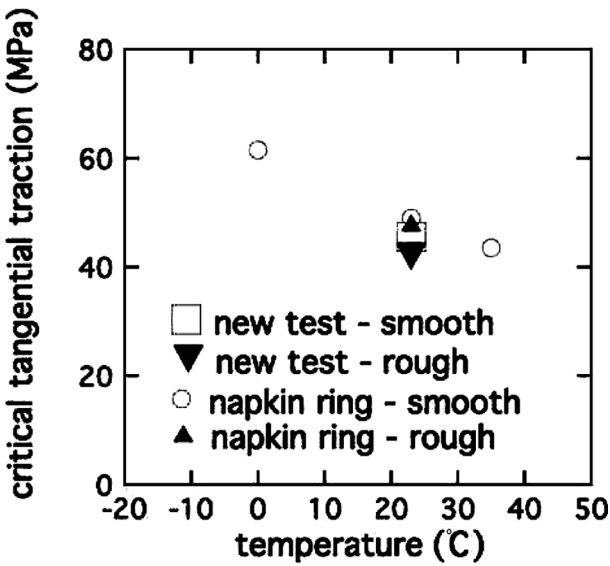

FIGURE 5 Temperature dependence of the critical tangential traction for debonding using the saucer and napkin-ring geometries with either polished or sand-blasted surface finishes.

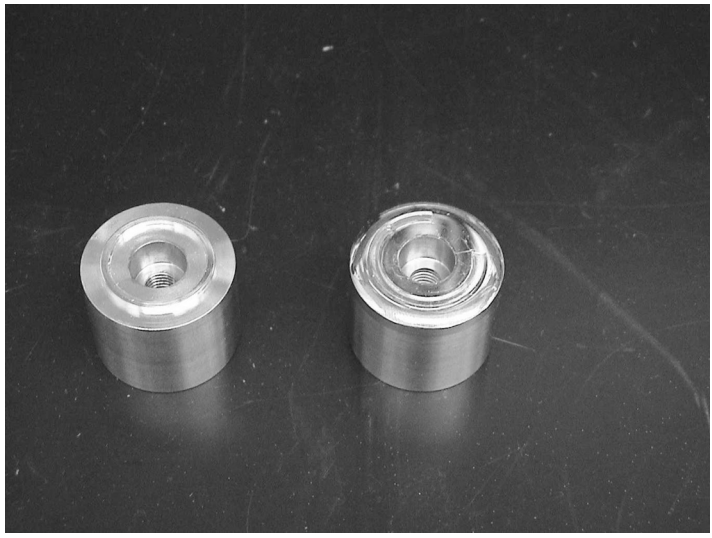

FIGURE 6 Failure surfaces of gold-plated napkin-ring samples.

relatively independent of temperature, the critical shear tractions vary by roughly 30% over a 40°C window. Most surprising was the insensitivity of either tensile or shear critical tractions on surface

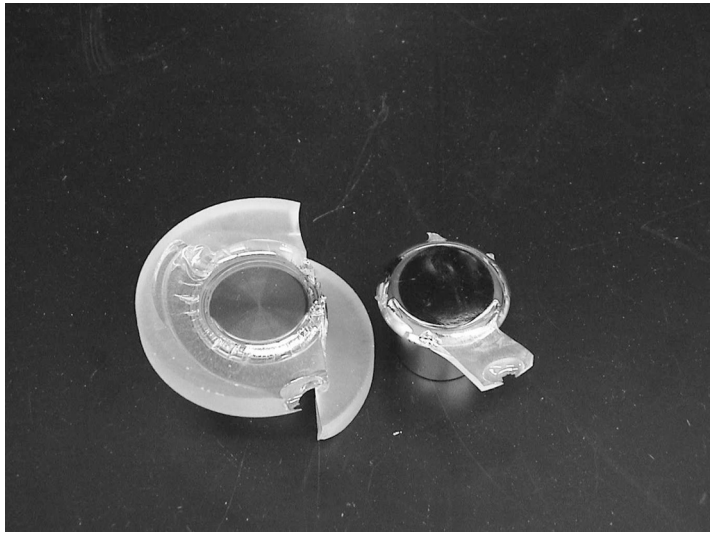

FIGURE 7 Failure surfaces of gold-plated saucer samples.

finish. Polishing or sand-blasting had little effect on the measured critical tractions for this epoxy in both the new saucer geometry as well as for the established napkin-ring geometry. Possible reasons for these observations were discussed in Ref. [4]. However, none of these deny a practical cleaning effect of sand-blasting in real applications.

Several new monotonically ramped tests were run at room temperature to determine the effect of curative, substrate, and filler level. The original plugs were fabricated from stainless steel for its strength. The stresses in the bulk epoxy at debonding were quite large, in some cases reaching yield. Therefore, it was interesting to examine a substrate for which adhesion was thought to be poor, for instance, gold. A nickel coating was first sputtered onto the polished faces of the stainless napkin ring or saucer followed by a gold layer. Debonding occurred at the epoxy–gold interface and not at any metal–metal interface (see Figures 6 and 7) in all four replicates of each test. The critical tractions

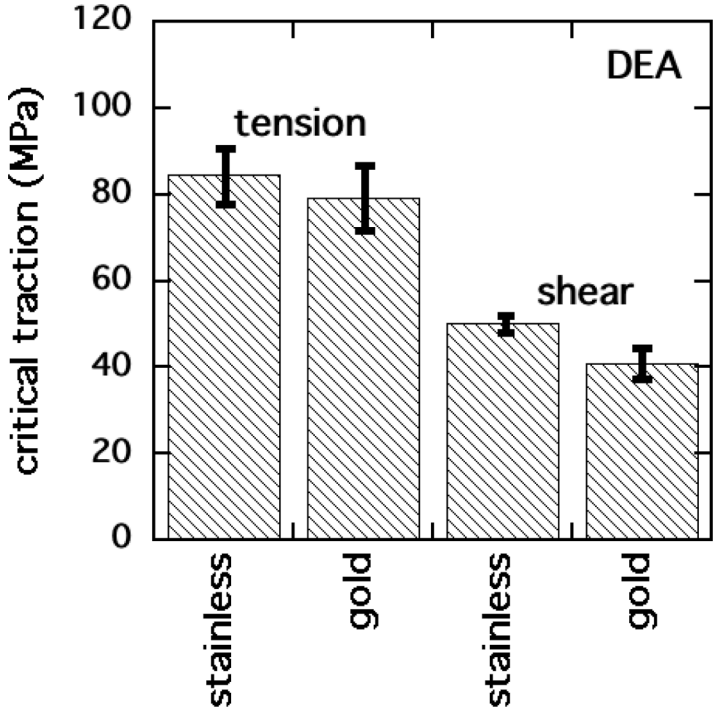

FIGURE 8 Comparison of the critical normal and tangential tractions for debonding from stainless steel or gold surfaces.

in both tension and shear showed little difference between the two substrates (Figure 8). The observations that gold and stainless steel exhibit similar critical tractions and that the critical tangential tractions are more than half the value of the critical tensile tractions are somewhat surprising. One might have guessed that interactions of the epoxy with such chemically inert substrates involved primarily simple van der Waals interactions, leading to a greater disparity between the tensile and shear critical tangential tractions. Remember that the absolute comparison between tensile and shear critical tractions was enabled by using the new test geometry where stresses at failure could be accurately determined.

In the next series of tests, the effect of epoxy curative was investigated in monotonically ramped tests. The DGEBA was now cured with a mixture of two aliphatic amines (Jeffamine D230, Huntsman, Salt Lake City, UT, USA, at 16.7 pbw and Ancamine 2049, Air Products Allentown, PA, USA, at 16.7 pbw). While DEA cross-links primarily through the epoxy alcohol reaction, the aliphatic amine mixture (J/A) cross-links through the traditional epoxy–amine reaction at a rate roughly 10 times as fast at the cure temperature of 90°C. Figure 9 shows that little effect was measured using stainless napkin rings (five replicates).

In the final monotonically ramped tests, the effect of fillers was investigated using the J/A-cured epoxy. Two types of alumina particles were used at two quite high loading levels: T64 (Alcoa, Pittsburgh, PA, USA) and AA18 (Sumitomo Chemical, New York, NY, USA). The T64 particles are quite polydisperse and irregularly shaped (Figure 10) whereas the AA18 particles are fairly round and monodisperse (Figure 11). Figure 12 shows that again little effect was measured using stainless napkin rings (four replicates). Perhaps this result is least surprising of all because filler particles are sterically excluded from the interface. For clarity, Table 1 summarizes the numerous monotonically ramped tests described previously.

3. TIMES-TO-FAIL FROM CREEP TESTS

In the following tests, stainless steel napkin rings glued together with the DGEBA/DEA epoxy were loaded to various torques less than critical, as measured in the constant ramp tests (roughly 34 N-m, giving a shear stress of 45 MPa). The torque was then held constant to assess if the samples would fail in time. Tests were performed at room temperature using a MTS (Eden Prairie, MN, USA) 858 Mini-BionixII servohydraulic test frame at ramp rates of 1.13 N-m/s (1.7 MPa/s for these napkin rings). Not only did the samples fail in time, but the

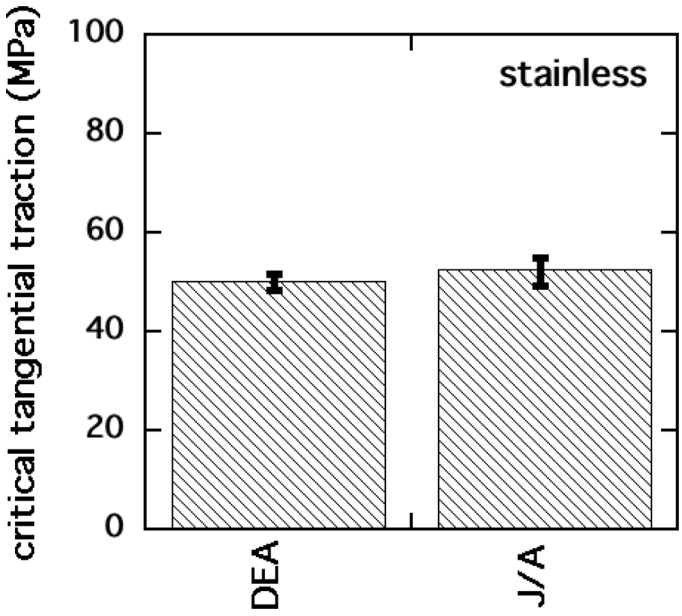

FIGURE 9 Comparison of the critical tangential tractions for debonding the DEA and J/A epoxies from stainless steel.

times-to-fail depended exponentially on the applied shear stress (Figure 13). Note that the times-to-fail are defined as the actual time at failure, which includes the ramp time.

To ensure that the observed time dependence arises from adhesive failure and not cohesive failure, notched three-point bend samples ($50 \times 13 \times 6.5$) mm of the DGEBA/DEA epoxy were tested in a similar fashion at room temperature. The critical failure load was determined in monotonically ramped tests using an Instron 1125 load frame at a ramp rate of 5 mm/min. Samples were then ramped to loads less than critical and held in time. Even at loads 95% of critical, the samples did not fail over a 3-day period. It therefore seems that the time dependence observed in the napkin-ring tests in this experimental window can be assigned to the initiation of adhesive failure.

Actual adhesive failures in real components are seen many times during thermal cycling. A robust design will not fail during the first excursion to low temperatures but will fail only after multiple cycles. This observation led us to test the time dependence of adhesive failure in oscillatory tests. Two types of load histories were applied to napkin rings at room temperature. In the first family of tests, a sinusoidal

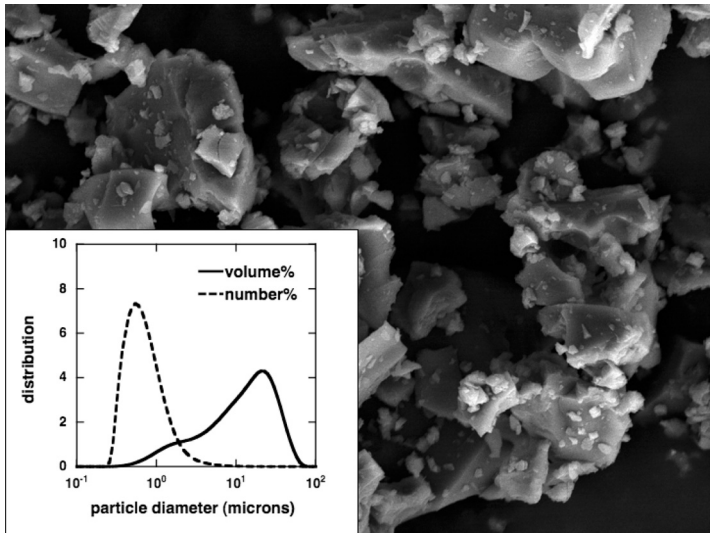

FIGURE 10 Micrograph and particle-size distributions of the T64 alumina.

torque of 0.1 Hz was applied ranging from 5 N-m to a subcritical value. In the second family of tests, a sinusoidal torque of 0.05 Hz was applied that oscillated between the positive and negative subcritical

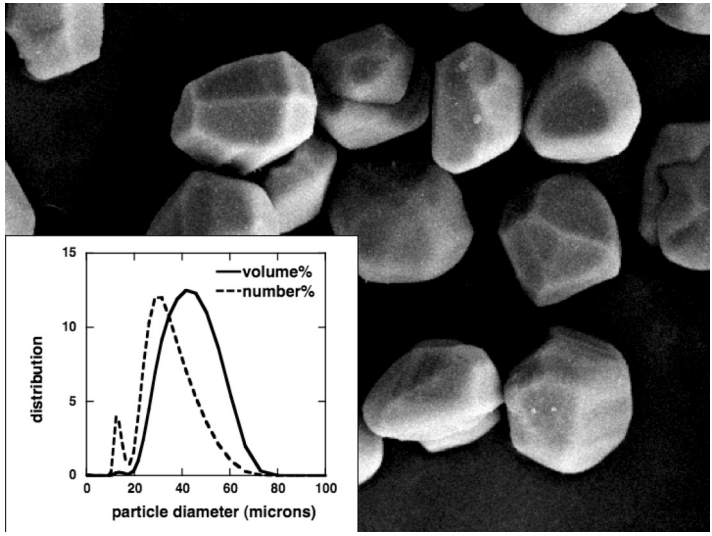

FIGURE 11 Micrograph and particle-size distributions of the AA18 alumina.

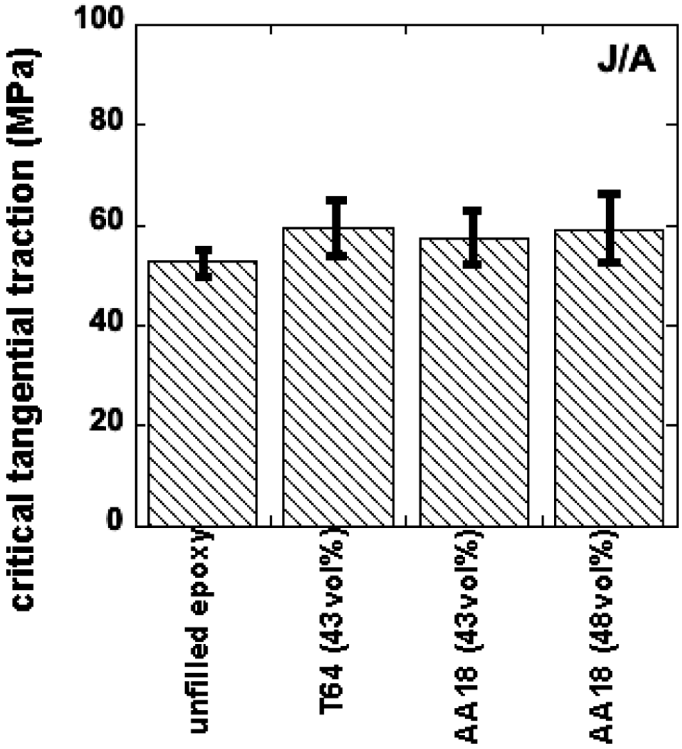

FIGURE 12 Dependence of the critical tangential traction on volume fraction of alumina filler (T64 and AA18) in the J/A epoxy.

TABLE 1 Summary of Monotonically Ramped Tests

Mode	Resin	Temp. range (°C)	Substrate	Surface finish	Filler
tension	DEA	–40 to 50	steel	polished	none
tension	DEA	23	steel	sand-blasted	none
tension	DEA	23	gold	polished	none
shear	DEA	0 to 35	steel	polished	none
shear	DEA	23	steel	sand-blasted	none
shear	DEA	23	gold	polished	none
shear	J/A	23	steel	polished	none
shear	DEA	23	steel	polished	T64 (43%)
shear	DEA	23	steel	polished	AA18 (43%)
shear	DEA	23	steel	polished	AA18 (48%)

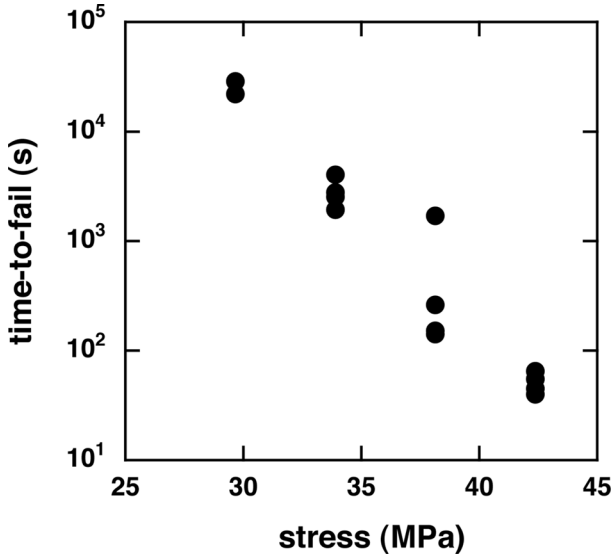

FIGURE 13 Times-to-fail from napkin-ring creep tests as a function of applied stress.

values. The tests were performed at different frequencies to make the dwell times near the maximum torque similar (see Figure 14). The data are shown in Figure 15. One might have guessed that the oscillatory times-to-fail would be considerably longer than the creep times-to-fail because the samples spend a smaller fraction of time at the high torques. Such behavior is seen for the single-sided tests. The double-sided tests surprisingly fail at roughly the same times as in creep. The difference between the times-to-fail between these two types of oscillatory tests cannot be attributed to the change in test frequency. As seen in Figure 16, the times-to-fail in the single-sided tests are independent of torque frequency.

The scatter seen in the data presented in Figures 13, 15, and 16 is noticeably large and should be explained. Even in the much simpler monotonically ramped tests, variability is observed in the failure load. In each creep test, a sample is loaded near but below this average failure load measured in the ramp tests. Therefore, each creep test not only exhibits a natural test-to-test variation but incorporates an additional variability due to the unknown failure load for that particular sample. Because the dependence of time-to-fail upon distance from the critical load is exponential, the effect of small variations in the critical load from sample to sample can be quite severe.

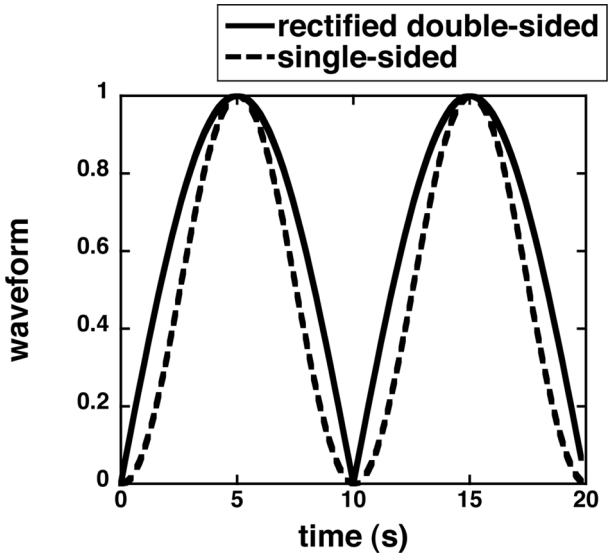

FIGURE 14 Time spent near the maximum stress in the single-sided and double-sided oscillatory tests is similar because the frequencies vary by a factor of two.

The oscillatory tests also suffer from this effect but seem to be even more inherently variable. Nevertheless, the exponential dependence of time-to-fail on applied load and the differences between creep and oscillatory loadings are so substantial that these results can be observed even with the significant scatter.

4. HISTORICAL THEORETICAL FRAMEWORKS

From a phenomenological viewpoint, two existing approaches may predict the observed time dependence of adhesive failure. The first approach has the flavor of the rupture of bonds between the epoxy and substrate. Decades ago, Bueche [7] proposed that the rupture of rubber cross-links is accelerated by mechanical work. Specifically, the underlying activation energy for thermal bond rupture in a first-order rate equation is modified by the applied work per cross-link

$$\frac{dc_{xl}}{dt} = -k_o e^{-(E_a - W/c_{xl})/RT} c_{xl}, \tag{1}$$

where c_{xl} is the cross-link molar concentration, k_o the rate constant, E_a the activation energy, and W is the applied work. For an elastic

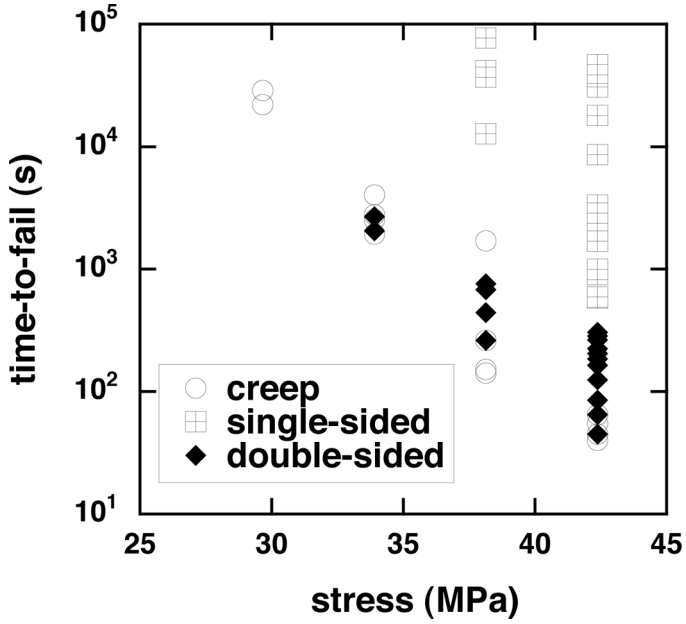

FIGURE 15 Comparison of the times-to-fail from napkin-ring tests in creep and single-sided and double-sided oscillatory tests.

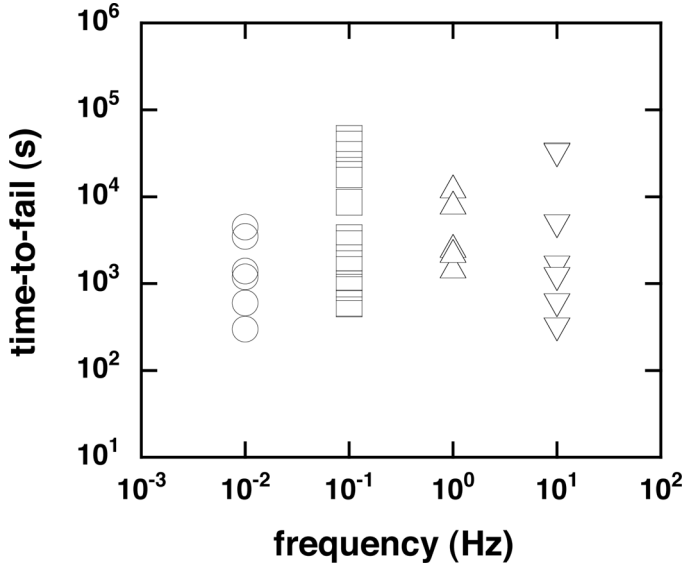

FIGURE 16 Times-to-fail in single-sided oscillatory tests appear independent of the frequency.

rubber, the equilibrium modulus, G_∞, is typically assumed to equal $c_{xl}RT$ so that Eq. (1) can be rewritten as

$$\frac{dc_{xl}}{dt} = -k_o e^{-E_a/RT} e^{\sigma^2/2G_\infty^2} c_{xl} \equiv -k_A \exp\left(\frac{\sigma^2}{2G_\infty^2}\right) c_{xl}. \quad (2)$$

For large constant applied loads, the solution to Eq. (2) for the time at which all cross-links are broken, t_f, given by

$$t_f = \frac{\sigma^2}{2k_A G_{\infty_o}^2} \exp\left(\frac{\sigma^2}{2G_{\infty_o}^2}\right), \quad (3)$$

where G_{∞_o} is the initial equilibrium modulus. Equation (3) states that the time-to-fail is exponentially dependent upon the applied load.

Because this exponential dependence of the adhesive time-to-fail on applied torque was observed in Figure 13, this type of formalism may offer quantitative predictions for debonding. Certainly, the stress per cross-link must be modified to "traction, τ, per surface bond, c_b." Note that the definition of a surface bond is purposefully

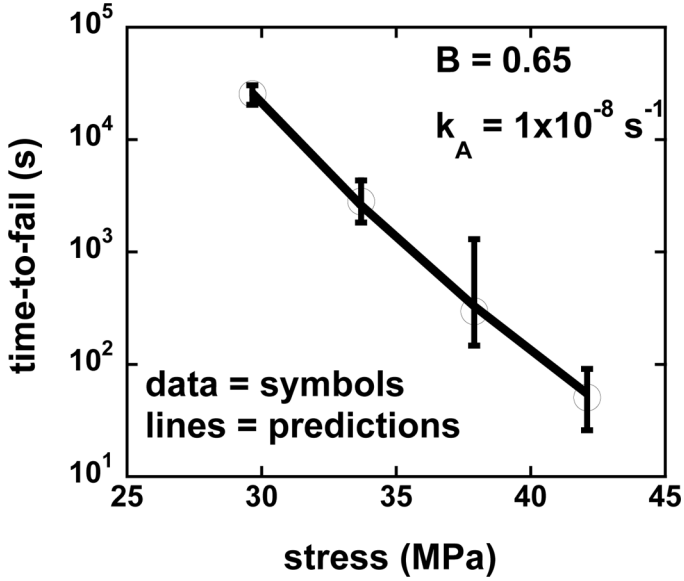

FIGURE 17 Times-to-fail from creep tests can be predicted quite well using the bond breakage model.

fuzzy to include interactions beyond simple covalent bonds. Without losing rigor but without undue physical interpretation, Eq. (3) can be recast for adhesive failure as

$$\frac{dc_b}{dt} = -k_A \exp\left(\frac{\tau^2}{Bc_b^2}\right) c_b, \tag{4}$$

where B is a phenomenological constant. In the simple napkin-ring test, the magnitude of the surface traction is proportional to the applied shear stress. Figure 17 shows that the predictions of Eq. (4) can agree quite well with creep data for appropriate choices of the two adjustable constants.

Equation (4) can be applied directly to the oscillatory tests as well. One can guess that the predicted times-to-fail in these fatigue tests should be longer than for creep tests at equal maximum applied load because the time spent at large loads is less. Indeed, Figure 18 shows that the predicted times-to-fail for the single-sided tests are an order of magnitude larger than for the creep tests. However, the measured times are roughly two orders of magnitude larger. Even more

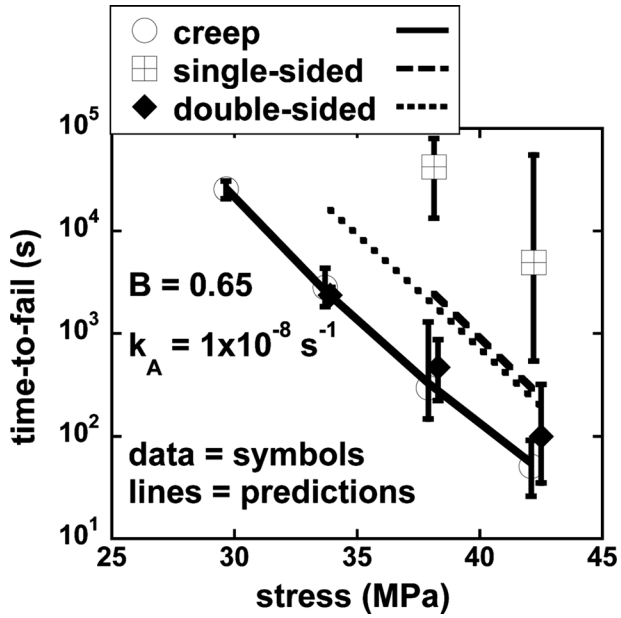

FIGURE 18 Times-to-fail from oscillatory tests are not predicted as well using the bond breakage model.

disturbing is the observation that the double-sided predictions are also an order of magnitude larger than the predicted creep times-to-fail whereas the experimental data for the two tests overlay.

A competing approach is based on accumulation of damage, D, and invokes the picture of growing surface flaws. A typical continuum damage evolution equation has been directly extended for use at surfaces [8]:

$$\frac{dD}{dt} = \left(\frac{J_2}{\beta}\right) D^{1-\beta} \qquad \text{such that } D = \left[\int_0^t ds\, J_2(s)^\beta\right]^{1/\beta}, \tag{5}$$

where $J_2 \equiv \sqrt{\underline{\underline{\sigma}} : \underline{\underline{\sigma}}}$.

Unlike the former approach, a critical value of damage must be defined here that indicates the initiation of failure. The solution for creep is trivial:

$$t_f = \left(\frac{D_c}{J_2}\right)^\beta \approx \left(\frac{D_c}{\sigma_s}\right)^\beta \text{ in shear.} \tag{6}$$

From Figure 19, the napkin-ring creep data are fit well by Eq. (9), albeit with an unusually large value of $\beta = 18.9$. Such large exponents often hint that the assumed power law relationship is fundamentally

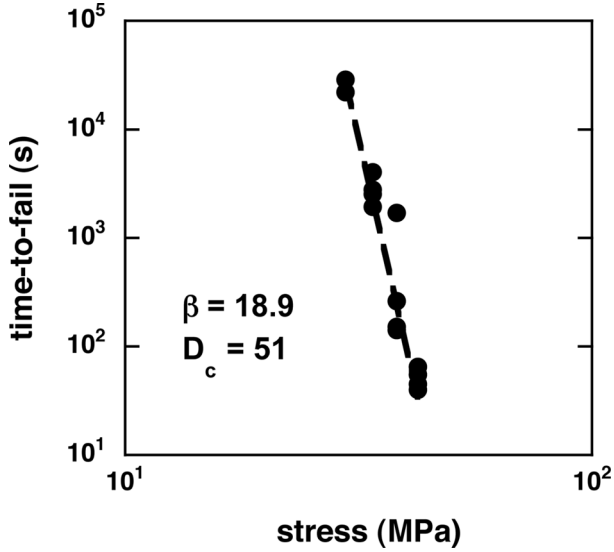

FIGURE 19 Times-to-fail from creep tests can be predicted quite well using the damage model.

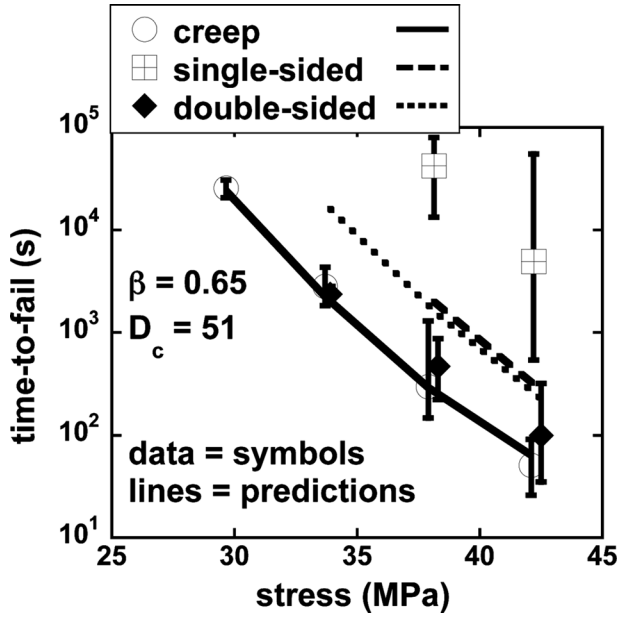

FIGURE 20 Times-to-fail from creep tests are not predicted as well using the bond breakage model.

incorrect. In this case, the experimental data seem to follow an exponential relationship more naturally. Nevertheless, the damage evolution law in Eq. (5) can be integrated numerically to predict the failure times in oscillatory tests as well (Figure 20). These predictions are very similar to those seen in the previous formalism of Eq. (4).

5. CONCLUSIONS

If a test geometry yields well-defined stresses at the initiation of debonding, quantitative analysis of the critical tractions can proceed. Only a few geometries (napkin-ring, cruciform, saucer) fulfill this requirement. The gross stress concentration in most historical tests (butt tensile, lap shear) casts doubt on the precise connection between the loads at failure and critical tractions. Many experimental results from tests with well-defined stresses, however, may differ from intuition gathered in the more conventional, historical geometries. It is important to stress that the following results have been established for a few epoxies, and thermoplastics may show differences:

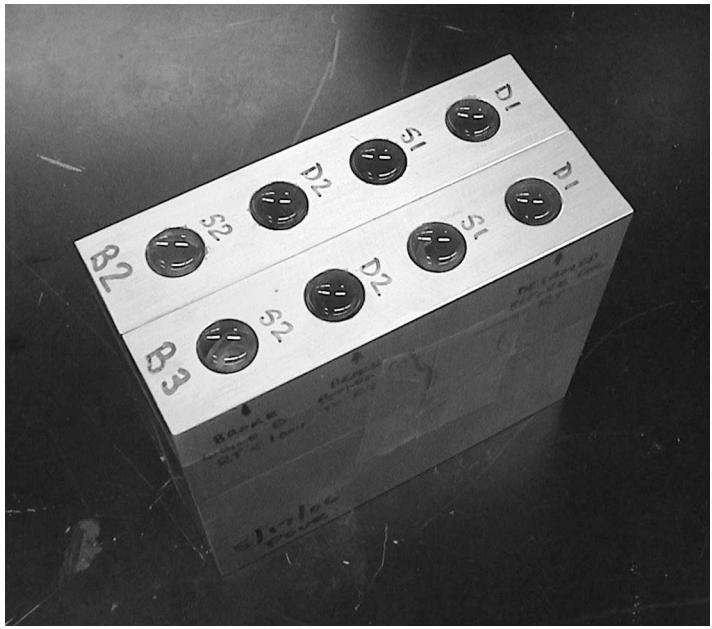

FIGURE 21 Photograph of the test geometry used to initiate adhesive failure by thermally generated stresses arising from mismatches in coefficients of thermal expansion.

1. The critical shear and tensile tractions from constant ramp tests are similar.
2. Surface roughness is fairly unimportant.
3. Substrates typically supposed to be fairly inert chemically produce critical tractions approaching the yield stress of epoxies.
4. Adhesive times-to-fail in creep tests are quite sensitive to the applied load.
5. Accurate predictions of the difference between times-to-fail in creep and oscillatory stress tests are difficult.

Nevertheless, some interesting and practical conclusions are apparent for these systems. It is clear that the initiation of adhesive failure is inherently time dependent. We have demonstrated similar behavior in simple, thermally driven tests (Figure 21). Here, cylindrical wells of various depths but constant diameter with rounded bottoms were machined into an aluminum block. Epoxies cured in deep wells failed at higher temperatures than epoxies cured in shallow wells. Interestingly, samples with wells of intermediate depth survived ramped

cooling to room temperature and failed after a hold of several hours at room temperature. This time dependence can also explain why components sometimes fail in thermal cycling tests not on the first excursion to the lowest temperature but only after multiple cycles. The research pursued in the studies described begins to develop the capability for quantitative prediction of adhesive failure in these somewhat realistic geometries.

It is also apparent that single-sided oscillatory tests take much longer to fail than simple creep tests. This point has practical significance because it provides definition for accelerated aging tests of thermoset debonding. Thermosets are almost always cured at high temperatures and experience oscillatory thermal histories at lower temperatures. The stress loading therefore resembles the single-sided oscillatory tests performed in this study. From our results, tests that cool to a low temperature and hold at temperature will initiate debonding sooner than tests that thermally cycle between the lowest temperature and some higher temperature below the cure temperature. That is, dwell-at-temperature tests are more effective accelerated aging tests than thermal cycling tests.

REFERENCES

[1] Reedy, E. D. and Guess, T. R., *J. Adh. Sci. Tech.* **9**, 237–251 (1995).
[2] Bossler, F. C., Franzblau, M. C., and Rutherford, J. L., *J. Physics E* **1**, 829–833 (1968).
[3] Tandon, G. P., Kim, R. Y., Warrier, S. G., and Majumdar, B. S., *Composites: Part B* **30**, 115–134 (1999).
[4] Adolf, D. B., Chambers, R. S., Stavig, M. E., and Kawaguchi, S. T., *J. Adhesion* **82**, 63–92 (2006).
[5] Caruthers, J. M., Adolf, D. B., Chambers R. S., and Shirkande, P., *Polymer* **45**, 4577–4597 (2004).
[6] Adolf, D. B., Chambers, R. S., and Caruthers, J. M., *Polymer* **45**, 4599–4621 (2004).
[7] Bueche, A. M., *J. Polymer Sci.* **19**, 275–284 (1956).
[8] Richardson, D. E., McLennan, M. L., Anderson, G. L., Macon, D. J., and Batista-Rodriguez, A., *J. Adhesion* **79**, 157–174 (2003).